

EFFECT OF PARTICLE SIZE DISTRIBUTION ON EXPLOSION RESISTANCE DURING HEATING OF ALUMINA CASTABLE BONDED BY HYDRATABLE ALUMINA

Zhanmin Wang*, Huan Wang, Haixia Feng, Yingnan Cao, Xiying Cao
State Key Laboratory of Advanced Refractories, Sinosteel LIRR, China

ABSTRACT

Effect of weight ratio of aggregate to fine on the explosion resistance during heating of alumina castables bonded by hydratable alumina was investigated with white fused alumina, hydratable alumina, reactive alumina and microsilica as the raw materials. The results showed that when aggregate contents increased, mechanical properties at room temperature of the specimens after drying at 110°C for 24 h gradually increased and that decreased after firing at 1400°C for 3 h; the bulk density both after drying and firing increased slightly, and apparent porosity decreased; air permeability for green and drying at 110°C increased at beginning and then decreased, the air permeability and average pore size of the specimens heat treated at 1400°C for 3h increased gradually; the explosion resistance increased first and then decreased, and which reached the best when the mass ratio of aggregates to fines is 68:22.

Key words: Alumina castable; Explosion resistance; Particle size distribution; Hydratable alumina; Air permeability

1 INTRODUCTION

The alumina cement is widely used in the refractory castables due to its easy use, relatively higher properties and stable performance. However, as the high content of CaO in castables containing cement, the high temperature performance and service life still faced challenges especially for the Al₂O₃-SiO₂ system as low melting point liquid phases formed during service^[1-3]. Hydratable alumina shows excellent properties such as good

volume stability and high temperature performance, and will not produce a large amount of low melting point liquid phase when used at high temperature, making it a promising candidate for applications as a binder in castables. Nevertheless, the hydration products of hydratable alumina have low density and worm-like morphology, which can easily block pores and reduce permeability. Meanwhile, the hydration products formed a large amount of water vapor due to dehydrated rapidly at 300-500°C. Therefore, castables bonded by hydratable alumina often show poor explosive resistance during rapid heating.

There are two ways to prevent the explosion spalling of castable during heating^[4-7]: 1) control the maximum steam pressure in castable by using appropriate drying and heating system; 2) improve the air permeability of castable by adding anti-explosion agent to form gas channels or micro-cracks^[8]. It is difficult to establish an appropriate drying and heating system as castables and casting body are different. Therefore, the addition of anti-explosion agents are normally adopted to improve the explosion resistance of castables^[9-11]. In recent years, many efforts have been made to improve the permeability of refractory castables to prevent the explosion spalling during heating. Various additives have been adopted, such as fibers, aluminum powder, Azoformamide and aluminum lactate, but few literatures indicated the explosion resistance of castables with particle size distribution of the castables. Effects of weight ratio of aggregates to fines on explosive resistance of WFA based castables bonded by hydratable Al₂O₃ was investigated in present paper.

This UNITECR 2022 paper is an open access article under the terms of the [Creative Commons Attribution License, CC-BY 4.0](https://creativecommons.org/licenses/by/4.0/), which permits use, distribution, and reproduction in any medium, provided the original work is properly cited.

2 EXPERIMENTS

Chemical compositions of WFA, reactive alumina ($d_{50}=1.198\ \mu\text{m}$) and microsilica ($d_{50}=0.268\ \mu\text{m}$) as the raw materials for experiments are shown in Table I. Hydratable alumina ($d_{50}=2.4\ \mu\text{m}$, $\text{Al}_2\text{O}_3\geq 99.6\%$) and sodium hexametaphosphate were used as the binder and deflocculant respectively.

Table I Chemical composition of raw materials

	wt/%				
	Al_2O_3	SiO_2	Fe_2O_3	K_2O	Na_2O
WFA	99.4	0.05	0.15		0.2
Microsilica	0.4	96.77	0.1	0.26	0.29
Reactive alumina	99.38	0.13			0.19

The dry mixes by Table II were pre-mixing for 2-3 min, then dry mixing in mixer for 90 s and wet mixing for 150s after adding water. The specimens of $40\times 40\times 160\text{mm}$, $50\times 50\times 50\text{mm}$ and $\phi 50\times 50\text{mm}$ were prepared by vibrating-cast process. Curing at room temperature for 24h and drying at 110°C for 24h, the specimens were fired in air at 1400°C for 3h.

Table II Formulations of specimens

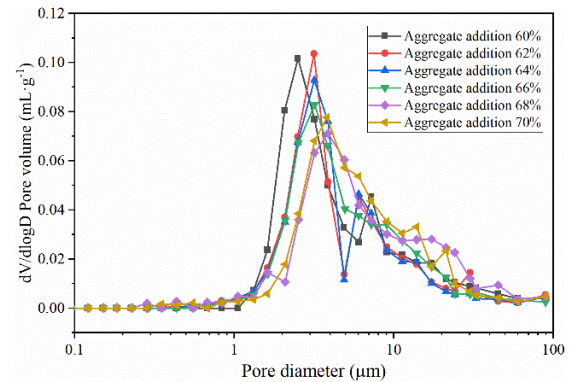
Raw materials	wt/%						
	A	B	C	D	E	F	
WFA	5-3 mm	15	16	17	18	19	20
	3-1 mm	30	30	30	30	30	30
	$\leq 1\text{ mm}$	15	16	17	18	19	20
	$\leq 0.074\text{ mm}$	30	28	26	24	22	20
Microsilica	2	2	2	2	2	2	
Reactive Al_2O_3	3	3	3	3	3	3	
Hydratable Al_2O_3	5	5	5	5	5	5	
SHP	0.2	0.2	0.2	0.2	0.2	0.2	
Water addition	5.3	5.1	4.9	4.8	4.7	4.5	

The permeability of specimens was tested by GB/T 3000-1999. Pore size and distribution of specimens was tested by Mercury porosimeter. Explosive spalling resistance of specimens was tested by the specimens of $50\times 50\times 50\text{mm}$ according to GB/T 36134-2018.

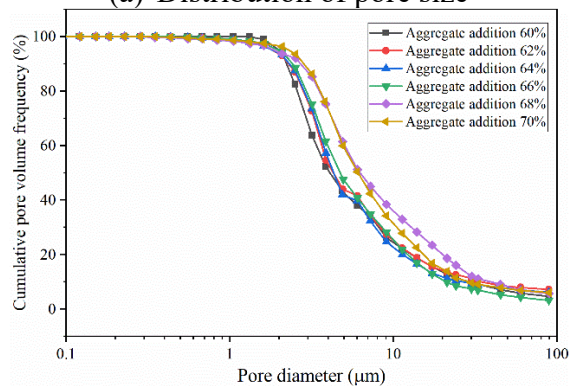
3 RESULTS AND DISCUSSION

3.1 Distribution of Pore Sizes

Fig. 1 gives the pore size distribution and cumulative percentage of specimens with different aggregate contents after heat treatment at 1400°C for 3h.



(a) Distribution of pore size



(b) Cumulative percentage of pore size

Fig. 1 Distribution of pore size of specimens with different aggregate contents after heat treatment at 1400°C for 3h

As shown in Fig. 1, when the aggregate content increased, the peak values in $1\text{-}10\ \mu\text{m}$ gradually decreased and the peak values with more than $10\ \mu\text{m}$ size increased, which indicated that the amount of $\square 5\ \mu\text{m}$ pores decreased, and the amount of $\square 8\ \mu\text{m}$ pores increased with the

aggregate contents changing from 60 wt% to 70 wt%. With aggregate contents increasing, the curves moved right, which showed that the average pore size increased. Some matrix powders filled the gaps between the aggregate particles, some covered on the surface of aggregate particles, and the rest increased the distance between the aggregate particles^[12]. Therefore, with aggregates increasing and fines decreasing, pore size increased as the gaps between aggregate particles were not fully filled.

3.2 Air Permeability

Air permeability values of specimens after demoulding, drying and heat treatment are shown in Table III. As shown in Table III, the values of specimens after demoulding and drying first increased and then decreased with the aggregate amount increasing. When aggregate content was 66 wt%, the air permeability values increased to about 0.22 and 0.26, respectively. The values of air permeability of specimens heat treated at 1400°C for 3h remarkably increased with aggregate content.

Table III Air permeability

(10 ¹⁵ /m ²)	A	B	C	D	E	F
Demoulding	0.10	0.09	0.12	0.22	0.17	0.08
110°C /24 h	0.17	0.16	0.21	0.26	0.23	0.12
1400°C /3 h	90.9	94.6	98.3	124.9	136.4	164.4

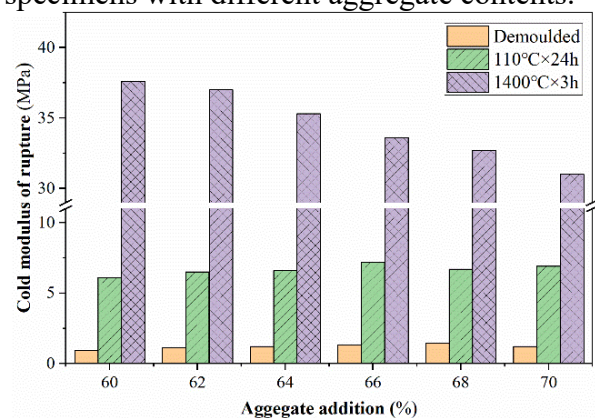
The water addition is also a key factor affecting air permeability of castables. The more water addition, the more air permeability is. It can be concluded that the weight ratio of aggregates to fines greatly affected the air permeability by Table III.

For the specimens demoulded and drying at 110°C, the air permeability increased with aggregate contents increasing when it was less than group D. It is believed that the pore content between aggregate particles play a key

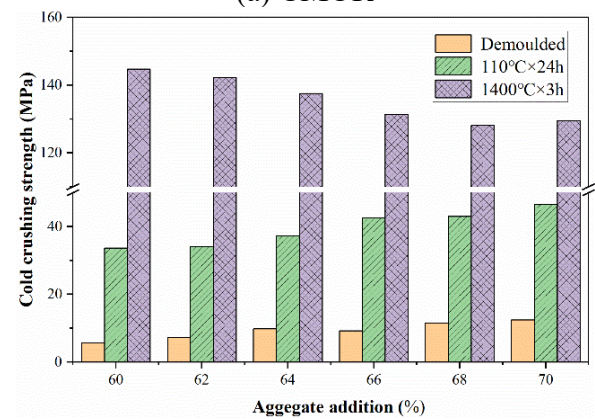
role for the permeability. However, when the aggregate content was more than group D, the permeability gradually decreased with addition decreased, which is believed that effect of water addition on air permeability plays a leading role instead of aggregate. For specimens after heat treatment at 1400°C, the permeability markedly increased because of the removal of bonded water and defects by sintering, which resulted in connectivity of the pores.

3.3 Physical Properties

Fig. 2 shows CMOR and CCS of specimens with different aggregate contents.



(a) CMOR



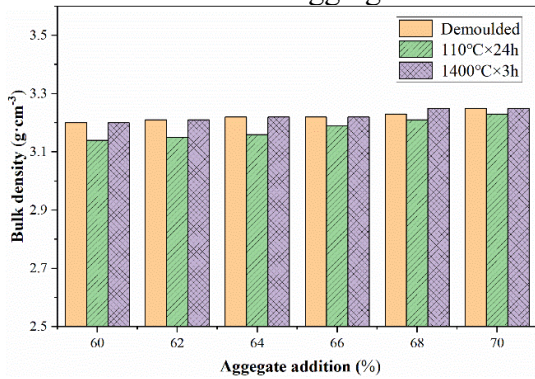
(b) CCS

Fig. 2 CMOR and CCS of specimens with different aggregate contents

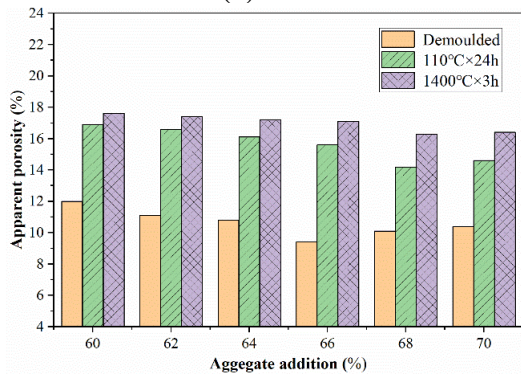
It showed that CMOR of demoulded and dried specimens kept almost same level and CCS increased gradually with aggregate contents increasing, due to the formation of

supporting skeleton by aggregates. While, CMOR and CCS of specimen heated at 1400°C for 3h decreased gradually with aggregates content increasing. The results indicated that increase of aggregates was detrimental to the strength of the fired specimens. As aggregate content increased, the average pore size of the sintered specimens increased gradually and caused the decrease of the sintered strength

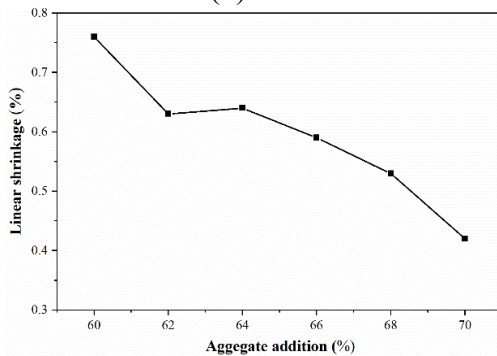
Fig. 3 shows BD, AP and PLC of specimens with different aggregate contents.



(a) BD



(b) AP



(c) PLC heat treated at 1400°C for 3h

Fig. 3 BD, AP and PLC of specimens with different aggregate contents

It is found by Fig. 3 that BD increased and AP decreased with the aggregate content increased. It is well-known that the more aggregate and the less water addition, the lower porosity of the castables would be after drying. This is consistent with the results of air permeability. PLC of specimens decreased with the aggregate contents increased because the fine contents decreased and the sintering performance of the specimens decreased.

3.4 Explosive Spalling Resistance

The results of the explosive spalling test with different aggregate contents at different temperatures are shown in Table IV. It can be seen that the specimens of group A did not explode when the furnace temperature was 450°C, but did when it was 500°C, and the explosion time was 303s. The anti-explosion temperature of group A is 450°C. Group B and C did not explode at 450°C, but did at 500°C in 442s and 520s respectively. So the anti-explosion temperatures of both B and C were 450°C. Specimens of group D and E did not explode at 500°C, but did at 550°C in 325s and 450s respectively. Then the anti-explosion temperatures of both D and E were 500°C. The anti-explosive temperature of group F was 450°C, and the explosion time was 502s at 500°C.

Table IV Explosive spalling test results of specimens with different aggregate contents at different temperatures

°C	A	B	C	D	E	F
550	××	××	××	××	××	××
500	××	O×	O×	OO	OO	××
450	OO	OO	OO	--	--	OO

(-) Untested (O) Not explosive (×) Explosive

Figure 4 shows photographs of burst specimens with different aggregate contents after explosive spalling test at different

temperatures. It can be seen that there was little difference between group D and E. However, the explosion resistance of group E was better than that of group D compared by the explosion time. In terms of explosion time, the explosion resistance of group A, B, C and F were as follows: $C > F > B > A$. It can be also found that the size of burst particles of specimens of group F and C were larger than those of group B and group A. The explosion time of group F was shorter than that of group C. So, the explosion resistance is summarized from the best to the worst as: $E > D > C > F > B > A$.

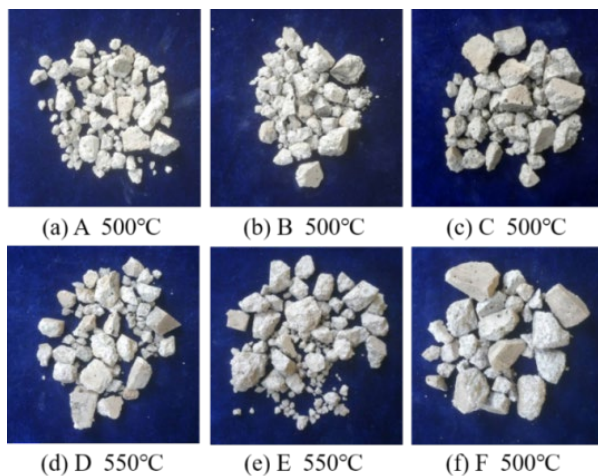


Fig. 4 Photographs of burst specimens of with different aggregate contents at the burst temperatures

The air permeability or densification, water addition and strength of the castables may affect the explosion resistance. The better the permeability is, the water-vapor formed by evaporation can escape faster, which slows down the accumulation of water vapor, and the explosion resistance would be better. As the aggregate contents increase, the permeability of castables tends to increase. Meanwhile, the explosion resistance tends to increase with the water content decrease. When aggregate content exceeds a certain level, permeability tends to decrease, then the explosive resistance will be deteriorating.

3 CONCLUSIONS

With the aggregate content increase, the mechanical properties of the specimens after demoulding and drying at 110°C gradually increase, while the mechanical properties of the specimens heat treated at 1400°C for 3h gradually decrease, the bulk density increases slightly, and the apparent porosity decreases. The air permeability after demoulding and drying at 110°C increases first and then decreases, the air permeability and the average pore size of the specimens after heat treatment at 1400°C increases gradually. Curing at room temperature for 12 hours, the explosion resistance of specimens increases first and then decreases. When the weight ratio of aggregate to fine is 68:22, the specimens show the best explosion resistance performance.

REFERENCES

1. M. F. Cai, J. H. Nie, G. H. Yin, *et al*, "Influence of Anti-explosive Agent on Performance of Corundum-spinel Castables", *Journal of Ceramics*, 38(6) pp 862-867 (2017).
2. X. J. Yang, Z. M. Wang, X. Y. Cao, *et al*, "Evaluation Methods for Resistance to Explosive Spalling of Dense Refractory Castables", *Refractories*, 52(2) pp 99-103 (2018).
3. N. N. XU, Y. B. LI, S. J. LI, *et al*. "Hydration Mechanism and Sintering Characteristics of Hydratable Alumina with Microsilica Addition", *Ceramics International*, 45(11) pp 13780-13786 (2019).
4. C. Q. Xie, "Research and Application of High Technology Castable Construction and Anti-explosive Sichuan Metallurgy", 25(2) pp 26-29 (2003).
5. G. Q. Wan, W. X. Cheng, "Effects of some Factors on Spalling Resistance of Al_2O_3 -SiC-C Castables", *Refractories & Lime*, 43(5) pp 10-13 (2018).
6. Z. Q. Wang, X. C. Li, B. Q. Zhu, *et al*, "Analysis on Mechanism of Explosive Spalling Resistance of Aluminum Powder on Ladle Corundum-based Refractory Castable",

Ceramics International, 2020, 46(11) pp 18958–18964 (2020).

7. J. J. Chen, Z. M. Wang X. Y. Cao, *et al*, “Study on Relationship Between Pore Structure Parameters and Permiability of Corundum-based Low Cement Castables”, Refractories, 52(2) pp 114-117 (2012).

8. Y. F. Liu, Y. Ding, F. Gao, “Influence of Vesicant on Anti-explosion Property and Strength of Quick Drying Castables Used for Iron Runner”, Rare Metal Materials and Engineering, 40(1) pp 159-161 (2011).

9. Y. L. Li, H. Z. Zhao, Z. A. Han, *et al*. “Enhancement and Explosion-proof Mechanism of Aluminum Fiber Addition in Al₂O₃–SiC–C Castables for Iron Runner”, Ceramics International, 45(17) pp 22723–22730 (2019).

10. F. A. Cardoso, M. D. Innocentini, M. F. Miranda, *et al*, “Drying Behavior of Hydratable Alumina-bonded Refractory Castables”, Journal of the European Ceramic Society, 24(3) pp 797–802 (2004).

11. B. Q. Zhu, “Effect of Permeability and

Pore Size on Explosive Spalling and Slag Penetration Resistance of Magnesia Based Coatings for Tundish”, Research on Iron and Steel, 2000, 34(4) pp 7-9 (2000).

12. W. D. Xue, W. Song, J. L. Sun, *et al*, “Effect of Particle Size Distributions on the Properties of Castable”, Rare Metal Materials and Engineering, 2007, 36(S2) pp 366-368 (2007).

13. Q. L. Jia, F. B. Ye, X. Zhong, *et al*, “Influnce of Particle Size Distribution on Rheological Properties of Ultra-low Cement Alumina-based Castables”, Refractories, 38(3) pp 168-171 (2004).

14. Y. Zhao, Y. Jin, F. Guo, “Effect of Aggregates on Properties of Alumina-spinel Castsbles”, Refractories, 49(S2) pp 198-200 (2015).

Author’s address: Sinosteel LIRR, 43 Road, Luoyang, Henan, China 471039
E-mail: wangzm@lirrc.com